

This is the accepted manuscript made available via CHORUS. The article has been published as:

Optical model potential of $A=3$ projectiles for 1p-shell nuclei

D. Y. Pang, W. M. Dean, and A. M. Mukhamedzhanov

Phys. Rev. C **91**, 024611 — Published 18 February 2015

DOI: [10.1103/PhysRevC.91.024611](https://doi.org/10.1103/PhysRevC.91.024611)

Optical Model Potential of $A = 3$ projectiles for $1p$ -shell nuclei

D.Y. Pang,^{1,2} W.M. Dean,^{2,3} and A.M. Mukhamedzhanov²

¹School of Physics and Nuclear Energy Engineering,

Beihang University, Beijing 100191, China

²Cyclotron Institute, Texas A&M University, College Station, TX 77843, USA

³Bowdoin College, 8800 College Station/Brunswick, ME 04011-8488, USA

(Dated: January 14, 2015)

Abstract

A set of global optical potential parameters describing the $A = 3$ particles (^3He and ^3H) elastic scattering from $1p$ -shell nuclei, HT1p, is obtained by simultaneously fitting 118 sets of experimental data of ^3He and ^3H elastic scattering from ^9Be , ^{10}B , ^{11}B , ^{12}C , ^{13}C , ^{14}C , ^{14}N , ^{15}N , ^{16}O , ^{17}O and ^{18}O with incident energies from $4 \leq E \leq 118.5$ MeV and 24 sets of elastic scattering data with the ^6Li and ^7Li targets from $3 \leq E \leq 44$ MeV. HT1p is found to be superior to GDP08 [D.Y. Pang, P. Roussel-Chomaz, H. Savajols, R.L. Varner, and R. Wolski, Phys. Rev. **C79**, 024615 (2009)], which is a systematic potential designed for the heavy-target region, in reproduction of the angular distributions of elastic scattering cross sections of ^3He and ^3H from $1p$ -shell nuclei at energies below 100 MeV. At energies above 100 MeV, GDP08 is found to be better than HT1p.

PACS numbers: 24.10.Ht 25.10.+s 25.55.Ci 27.10.+h

I. INTRODUCTION

Systematic optical model potentials (SOMPs) are necessary inputs for direct nuclear reactions models, which are widely used in studies of nuclear structures and nuclear astrophysics. The importance of SOMPs in such studies are not only shown in cases when experimental data of elastic scattering cross sections are not available, but also in other works, such as systematic study of spectroscopic factors using, for example, (d, p) , (p, d) , and $(^3\text{He}, d)$ reactions. In such studies, systematically consistent results can only be obtained when SOMPs are used [1–3]. When exploring into unknown regions, either in nuclear chart that are far away from the β -stability line or in some key nuclear reactions in nuclear astrophysics which are very difficult or even not possible to measure directly with current facilities, reliable predictions of theoretical models, or at least the understanding of the uncertainties of the various theoretical models are crucial [4]. Uncertainties in optical model potentials consists one of the main sources of uncertainties in predictions of direct nuclear reactions (see, e.g. Ref.[5]). It is thus important to develop OMPs, which are obtained by optimizing descriptions of scattering observable, usually angular distributions of elastic scattering cross sections (ADXSECs), over a wide range of incident energies and nuclear masses. Systematic OMPs obtained in this way minimize the uncertainties of OMPs as inputs in direct nuclear reactions.

Over the many years, a lot of efforts have been made in developing SOMPs for nucleon ($A = 1$) [6–9], deuteron ($A = 2$) [10–13], ^3H and ^3He ($A = 3$) [14–18], alpha-particles ($A = 4$) [19–22], and heavy ions ($A \geq 6$) [23–25]. However, most of these potentials are based on analysis of ADXSECs of projectiles from heavy targets with atomic masses of, typically, $A_T \geq 30$. It is well-known that the systematic behaviour, namely, the energy- and target-mass-dependence of depth and geometry parameters of OMPs are quite different between heavy and light nuclei regions [16, 22, 26]. Although these SOMPs are very often extrapolated to nuclei with $A_T < 30$ [1, 27, 28], they are not optimized for those regions. It has been found that some modification of these potentials should be made in order to best reproduce experimental data with light particles [29]. Systematic OMPs for light nuclei should be developed whenever possible. Besides such practical purposes, a SOMP established in the light-target region, which are not as much studied as in the heavy-target region, will quantify the differences in the behaviour of SOMPs between light- and heavy-mass regions,

and will be helpful in finding a proper parameterization that aims to cover both mass regions. The relative difference in the target masses are much larger in the light-mass region than that in the heavy-mass region, for example, the difference in masses of ^9Be and ^{10}B is 10% while that between ^{40}Ca and ^{41}Ca is only 2.5%. The differences in energy-level densities among light nuclei are also larger than that of the heavy ones. It is thus questionable if a systematic potential can be obtained for a light-mass region. Nevertheless, some successful pioneer work have been made for the $1p$ -shell nuclei, namely, for nuclei with atomic numbers ranging from 3 to 8, for protons and neutrons [30] and heavy-ions [31].

In this paper, we report a SOMP of ^3He and ^3H on $1p$ -shell nuclei, designated as HT1p (H and T being initials of helion and triton, respectively). This potential is obtained by simultaneously fitting 118 sets of ADXSEC data of ^3He and ^3H elastic scattering from ^9Be , ^{10}B , ^{11}B , ^{12}C , ^{13}C , ^{14}C , ^{14}N , ^{15}N , ^{16}O , ^{17}O , and ^{18}O . The incident energies covered by these experimental data are from 3.7 MeV to 118.5 MeV. The potential for ^6Li and ^7Li are searched separately from the other $1p$ -shell nuclei with incident energies from 3 to 44 MeV. As we show in Section II B, the OMP parameters for these two nuclei differ significantly from the other $1p$ -shell nuclei. This may be attributed to their weak binding energies or ^3He or ^3H cluster structure.

This paper is organized as the following: the parameterization of the SOMP is introduced in Section II A; the resulting parameters are reported in Section II B with comparisons between optical model calculations and experimental data; discussions on the applicable energy ranges of HT1p and GDP08, and volume integrals of these potentials are given in Section III. Our conclusions are made in Section IV.

II. PARAMETERIZATION AND DETERMINATION OF THE SYSTEMATIC POTENTIAL PARAMETERS

A. Parameterization of HT1p

The parameterization of HT1p for the $1p$ -shell nuclei is the same as that of GDP08[16] except for the introduction of an energy-dependence parameter to the real potential radius. For this reason, we simply recapitulate the necessary equations and refer Ref.[16] for detailed discussions about this parameterization. The phenomenological optical model potential, as

a function of the radial distance between the center-of-masses of the projectile and the target nuclei, r , is defined as:

$$\begin{aligned}
U(r) = & -V_r f_{ws}(r, R_0, a_0) - iW_v f_{ws}(r, R_w, a_w) \\
& -iW_s(-4a_w) \frac{d}{dr} f_{ws}(r, R_w, a_w) \\
& +V_C(r),
\end{aligned} \tag{1}$$

where V_r , W_v , and W_s are depths of the real, volume-imaginary, and surface-imaginary parts, respectively. f_{ws} is the Woods-Saxon form factor:

$$f_{ws}(r, R, a) = \frac{1}{1 + \exp[(r - R)/a]}, \tag{2}$$

with R and a being the geometry parameters (radius and diffuseness) of the potential. V_r , W_v , W_s , have their associate R and a values, distinguished by their subscripts as is shown in Eq.(1). V_C is the Coulomb potential:

$$V_C(r) = \begin{cases} \frac{Z_P Z_T e^2}{r}, & (r \geq R_C) \\ \frac{Z_P Z_T e^2}{2R_C} \left(3 - \frac{r^2}{R_C^2}\right), & (r \leq R_C), \end{cases} \tag{3}$$

with Z_P and Z_T being the charge numbers of the projectile and targets nuclei, respectively and, R_C is the radius of the Coulomb potential, which is defined as $R_C = r_c A_T^{1/3}$ (A_T is the mass of the target in the atomic mass unit). It was found that the angular distributions of elastic scattering cross sections are not much sensitive to the values of Coulomb radius. In this work, we fix $r_c = 1.3$ fm for all target nuclei.

We parameterize the energy- and target-mass dependence of the depth and geometry parameters as the following:

1. The depth of the real part of nuclear potential is:

$$V_r = V_0 + V_e(E - E_C), \tag{4}$$

where E_C is the Coulomb correction to the incident energy, which is taken to be the average value of the Coulomb potential inside the nucleus[7, 10, 16]:

$$E_C = \frac{6Z_P Z_T e^2}{5R_C}. \tag{5}$$

Note that Eq. (5) imply a $Z_T A_T^{-1/3}$ term in the real potential that has been introduced in the previous works (see, e.g., Refs. [17, 18, 32, 33]).

2. The depth of the volume and surface imaginary potentials, W_v and W_s , respectively, are functions of the incident energy E :

$$W_v(E) = \frac{W_{v0}}{1 + \exp\left(\frac{W_{ve0} - (E - E_C)}{W_{vev}}\right)}, \quad (6)$$

$$W_s(E) = \frac{W_{s0} \pm W_{st}\varepsilon}{1 + \exp\left(\frac{(E - E_C) - W_{se0}}{W_{sew}}\right)}, \quad (7)$$

where $\varepsilon = (N_T - Z_T)/A_T$ is the isospin asymmetry of the target nucleus, the “+” and “−” signs are for ^3He and ^3H projectiles, respectively.

3. The radius of the real potential consists of the term that is proportional to $A_T^{1/3}$, the offset term, and the energy-dependence term:

$$R_0 = r_0 A_T^{1/3} + r_0^{(0)} + r_{0e}(E - E_C). \quad (8)$$

The energy dependence of the geometry parameters, which might not to be necessary in systematic potentials of nucleons [7, 8], was found necessary for composite particles, such as, deuterons [12] and α -particles [21], when a large range of incident energies is covered. The diffuseness parameter a_0 is assumed to be independent on target masses and incident energies.

4. The volume and surface imaginary potentials are assumed to have the same geometry parameters:

$$R_{wv} \equiv R_{ws} = R_w = r_w A_T^{1/3} + r_w^{(0)}, \quad (9)$$

and, like that of the real potential, the diffuseness parameters $a_{wv} \equiv a_{ws} = a_w$ are assumed to be independent on A_T and E . Addition of the energy dependent term, $r_{we}(E - E_C)$, to R_w has been attempted. It is found that r_{we} is not well determined by the experimental data included in this work, namely, its values was determined with an uncertainty that is larger than itself and addition of this parameter did not provide an apparent improvement to the description of the experimental data. Because of this, we do not include the energy dependence to the geometry parameters of the imaginary potentials in the current work.

Only experimental data of ADXSECs are used in this work and most of which do not cover backward angles. These data do not confine the spin-orbit potentials sufficiently well

[26]. Because of this, we do not include the spin-orbit potentials in our parameterization in this work. All energies quoted in the text, or in the equations, are projectile incident energies in the laboratory system.

B. Determination of the systematic OMP parameters for $1p$ -shell nuclei

Experimental angular distributions of elastic scattering cross sections are used to confine the SOMP parameters. The database consists of 118 sets of data for target nuclei of ^9Be , $^{10,11}\text{B}$, $^{12-14}\text{C}$, $^{14,15}\text{N}$, and $^{16-18}\text{O}$ with the incident energies from 3.7 to 118.5 MeV and 24 sets for ^6Li and ^7Li from 3 to 44 MeV. Because ^6Li and ^7Li are very weakly-bound with $^3\text{He}/^3\text{H}$ cluster structure, we would expect that the potential systematics with these isotopes do not consistent with the systematics established for other $1p$ -shell nuclei. Actually, this is confirmed by our results (see Table.II). Because of this, the potential parameters of ^6Li and ^7Li are searched separately. The coverage of target masses and incident energies of the data sets is depicted in Fig.1. More detailed information about the database is listed in Table I. All the data sets used in this work are digitized from their original papers except for ^3H elastic scattering on ^6Li at 3-10 MeV [34], which are taken from the nuclear database EXFOR[35].

The systematic OMP parameters are determined by the usual criteria of the minimum deviation of results of optical model calculations from the experimental data, which is defined as

$$Q^2 = \frac{1}{N} \sum_{i=1}^N \frac{[\sigma_i^{\text{exp}} - \sigma_i^{\text{th}}]^2}{\Delta\sigma_i^2}, \quad (10)$$

where N is the number of data points, σ_i^{exp} and σ_i^{th} are the experimental and theoretical differential cross sections, respectively, and $\Delta\sigma_i$ is the uncertainty of the experimental cross sections. Q^2 in literature is usually called χ^2 . However, as in CH89 and GDP08, we retain the notation of Q^2 because, as was discussed in Ref. [7], this value, which is estimated by simultaneously fitting many sets of experimental data from different sources with different assertions of uncertainties, does not obey the χ^2 distribution. Since different data sets measured by different groups using different facilities have different uncertainties, using reported experimental uncertainties in the global fitting may put some unreasonable weight to some specific data sets. Because of this, we assume a uniform uncertainty of 15% for all the

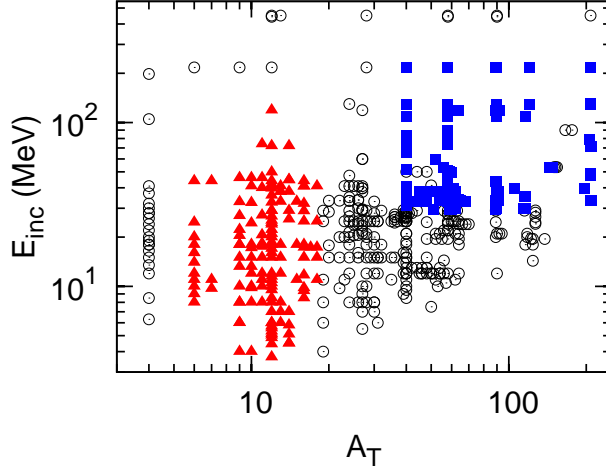


FIG. 1: (Color online) Incident energy and target mass distributions covered by the database of the angular distributions of the differential cross sections collected for ^3He elastic scattering from atomic nuclei. The squares represent those included in GDP08, the triangles are used for HT1p, and the circles are those unexplored by us.

data sets in the database. We allow variations of the normalization of the experimental data during the parameter fitting. Values of the parameters are determined using the computer code MINOPT [7], which is a combination of the optical model program OPTICS[36] and the multi-parameter minimization program, MINUIT[37]. It allows us to optimize the OMP parameters *simultaneously* by fitting a big set of experimental data which covers a large range of target masses and incident energies.

The details of fitting procedures are the same as those elaborated in Ref. [16] and we omit them in the present paper. The resulting SOMP parameters for the $A = 3$ particles with the $1p$ -shell nuclei are listed in Table.II. The parameter values of GDP08 are also shown for comparisons. The uncertainties of these parameters are determined with the bootstrap uncertainty analysis method [87], which simulates many repeated measurements of the data by creating new data sets of the same size as those in the original database using random sampling with replacement (see Ref. [7] for details of the bootstrap method). The parameter uncertainties are obtained with 1000 resamplings. The energy-dependence parameters of the imaginary potential, $W_{\text{ve}0}$, $W_{\text{ve}w}$, $W_{\text{vs}0}$ and $W_{\text{se}w}$ in Eq. 6, are found to be not well-determined by the experimental data included in this work. For example, when we allowed these four parameters to vary, we got $W_{\text{ve}w} = 2.08 \pm 3.18$ MeV and $W_{\text{se}w} = 71.9 \pm 74.3$

TABLE I: References for the data sets used in searching of the optical model parameters.

helium								
target	Elab	Ref	target	Elab	Ref	target	Elab	Ref
	8,9,10							
^6Li	11,12,14	[38]	^{12}C	8.5, 10	[39]	^{14}C	37.9	[40]
	16,18,20							
	24.6, 27	[41]		9.5, 10.5	[42]		44.8	[43]
				11.5				
	33.3	[44]		11	[45]		72	[46]
	44	[47]		12, 15	[48]	^{14}N	4.5, 7	[49]
^7Li	33.3	[44]		15	[50]		25.7, 29	[51]
	44	[47]		18, 20, 21	[52]		26.3	[53]
^9Be	4, 6, 8			18.6, 20				
	10, 15, 18	[54]		22.2, 23.9	[55]		44.6	[43]
	6, 8, 18	[56]		24.5, 25.3	[51]	^{15}N	11	[42]
				26.8				
	13.2, 20.4							
	22.2, 27	[57]		28.95	[58]		18	[59]
	32.8	[60]		29	[61]		33	[62]
	46.1	[47]		32.6	[60]	^{16}O	25	[63]
^{10}B	4, 8, 10							
	12, 15, 18	[64]		36, 42	[65]		28.9	[51]
	9.8	[66]		39.7	[67]		40.9	[68]
	11	[42]		40.9	[68]		41	[69]
	13.2, 17.2							
	24.3	[57]		41	[69]		44	[47]
	32	[70]		44	[47]	^{17}O	11	[42]
	41	[69]		49.8	[43]		17.3	[71]
	46.1	[47]		72	[72]		33	[73]
^{11}B	8, 15	[54]	^{13}C	6, 8	[74]	^{18}O	11	[42]
	10, 12, 18	[75]		12, 15, 18	[48]		11	[76]
	17.5, 40	[77]		33	[62]		15	[50]
	18.3, 20.6							
	27.2	[57]		37.9	[40]		17.3	[71]
	46.1	[47]		37.9	[78]		25	[63]
	74	[79]		41	[69]		33	[73]
^{12}C	3.7	[80]	^{14}C	10, 12				
				15, 18	[64]		41	[69]
	6	[74]		29	[51]			
triton								
target	Elab	Ref	target	Elab	Ref	target	Elab	Ref
	3, 4, 5							
^6Li	6, 7, 8	[34]	^{12}C	36	[81]	^{16}O	33	[82]
	9,10							
	17	[83]		38	[84]		36	[81]
^{12}C	20	[85]	^{13}C	38	[84]			
	33	[82]	^{14}C	72	[86]			

MeV, and Q^2 , with the number of free parameters increased from 12 to 16, only changed from 63.0 to 61.8. For this reason, we keep the values of these parameters to be the same as those in GDP08. Similarly, the volume absorption part and the energy dependence of the real potential radius for ${}^6,{}^7\text{Li}$ are ignored.

TABLE II: Values (P) and their uncertainties ΔP of the parameters in the systematic optical potentials for $A = 3$ nuclei. V_0 , V_e , W_{V0} , W_{S0} , W_{ST} , W_{ve0} , W_{vew} , W_{se0} , and W_{sew} are in MeV and r_0 , $r_0^{(0)}$, r_{0ae} , a_0 , r_w , $r_w^{(0)}$, and a_w are in fm.

	$1p$		${}^6,{}^7\text{Li}$		GDP08	
parameter	P	ΔP	P	ΔP	P	ΔP
V_0	155.1	1.6	80.1	7.7	118.3	1.3
V_e	-0.678	0.027	-0.61	0.21	-0.13	0.01
r_0	0.920	0.009	1.48	0.13	1.3	0.01
$r_0^{(0)}$	0.108	0.017	-	-	-0.48	0.05
r_{0ae}	0.0031	0.0002	-	-	-	-
a_0	0.792	0.002	0.590	0.044	0.82	0.01
W_{V0}	33.1	2.3	-	-	38.5	3.9
W_{S0}	21.8	0.6	25	10	35.0	1.1
W_{ST}	13.1	4.5	-	-	34.2	8.0
r_w	1.43	0.04	0.83	0.24	1.312	0.02
$r_w^{(0)}$	-0.16	0.10	-	-	-0.129	0.10
a_w	0.801	0.010	1.047	0.098	0.84	0.01
W_{ve0}	156.1	-	-	-	156.1	11.9
W_{vew}	52.4	-	-	-	52.4	8.2
W_{se0}	30.8	-	30.8	-	30.8	4.7
W_{sew}	106.4	-	106.4	-	106.4	8.0

It is interesting to compare the values of parameters of HT1p with that of CH89, which were determined for the heavy-target and, generally, higher energy region (see Fig. 1 for comparison). We can conclude that:

1. The depth of the real potentials are larger for the light targets than for the heavy targets. This is consistent with Trost *et al.* [26]. It would be interesting to see if microscopic theories of optical model potentials can explain this systematic difference between light and heavy targets.
2. The depth of the imaginary potentials for the light targets are smaller than for the heavy targets. This is also consistent with Trost *et al.* [26]. The systematically weaker absorption in the light-target region may relate to the fact that the average energy level densities in this region is smaller than that in the heavy-target region.
3. The radius parameter, r_0 , of the real potentials of light targets is much smaller than that of heavy targets, and the effective reduced radius parameter $r_0(1 + r_0^{(0)} A_T^{-1/3})$ depends oppositely on target-masses in these two mass regions. On the other hand, the radius parameter of the imaginary potentials for light targets are larger than that of heavy targets.

The parameters of ${}^6,{}^7\text{Li}$ show very different behaviour from the other $1p$ -shell nuclei. This may relate to weak-bounding nature of these two nuclei and their cluster structures. Of course, one should also note that these parameters with the Lithium isotopes are determined with a much smaller database and most of the data are in the low-energy region, which do not constraint the potential parameters sufficiently well. As expected, the deficiency of the database for the Lithium isotopes results in big uncertainties of the parameters, which are clearly shown in Table II.

III. DISCUSSIONS

A. Energy region of applicability of HT1p

In Figs. 2, 3 and 4 we show the comparison of the optical model calculations with the ADXSECs and the experimental data. Results obtained using GDP08 are also shown. Although the details of these comparisons can not be shown clearly for each single case, these figures suggest that, with respect to GDP08, which was determined by fitting the data for target masses $A_T \geq 40$, there is an overall improvement in reproduction of the experimental data with HT1p.

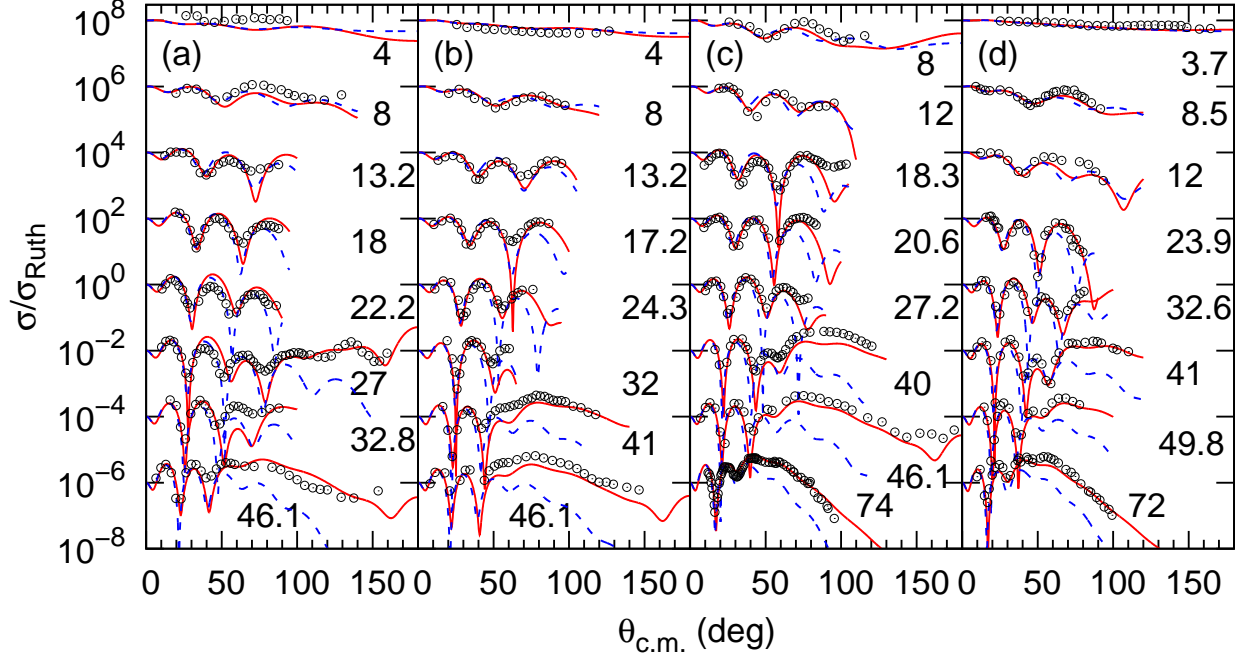


FIG. 2: (Color online) Optical model calculations of the angular distributions and their comparisons with the experimental data for ^3He elastic scattering from (a) ^9Be , (b) ^{10}B , (c) ^{11}B , and (d) ^{12}C . The cross sections are scaled by factors of 10^2 . The incident energies are indicated in the figures in unit of MeV. The solid and dashed curves are results of the optical model calculations with the systematic potential with $1p$ -shell nuclei and that with GDP08 [16].)

Since all of the experimental data included in this work have incident energies not exceeding 74 MeV (the only exception is $^3\text{He}+^{12}\text{C}$ scattering at $E = 118.5$ MeV), the present systematic potential focuses only on the low energy region for the $1p$ -shell nuclei. As we see from Figs. 2, 3 and 4, within such an energy region, this potential reproduces the elastic scattering cross sections well. However, for incident energies larger than 74 MeV (unfortunately, to our knowledge, there are no experimental data between 74 and 118 MeV), GDP08 is better than HT1p in reproduction of the ADXSECs. Success of GDP08 in reproducing the ^3He elastic scattering from light nuclei, which are very far away from the region where it is determined, such as ^6Li , ^9Be , and ^{12}C , at energies larger than around 100 MeV, are shown in Fig. 11 of Ref. [16]. This is illustrated again in Fig. 5, where we show the failure of HT1p compared to GDP08 in the reproduction of ^3He elastic scattering from ^{12}C at 118.5 and 217 MeV [33, 88]. The reason why GDP08 is still reliable for target masses as small as 6 at higher incident energies and its failure at low energies for the $1p$ -shell nuclei may be

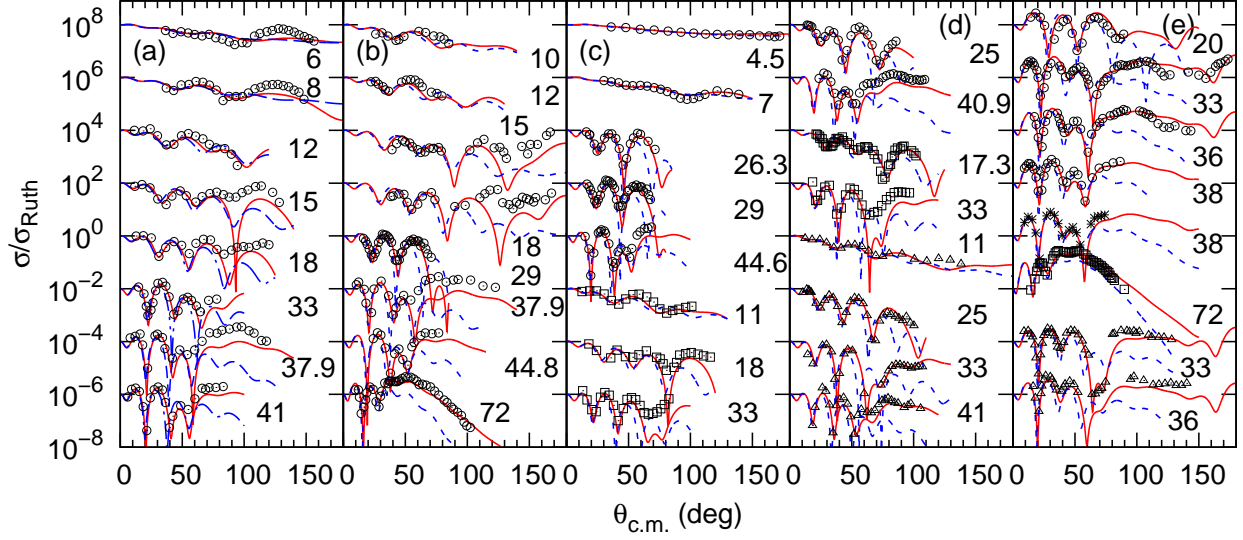


FIG. 3: (Color online) The same as in Fig. 2 but for ^3He elastic scattering from targets (a) ^{13}C , (b) ^{14}C , (c) ^{14}N (circles), and ^{15}N (squares), (d) ^{16}O (circles), ^{17}O (squares) and ^{18}O (triangles), and ^3H elastic scattering from targets of (e) ^{12}C (circles), ^{13}C (asterisks), ^{14}C (squares) and ^{16}O (triangles).

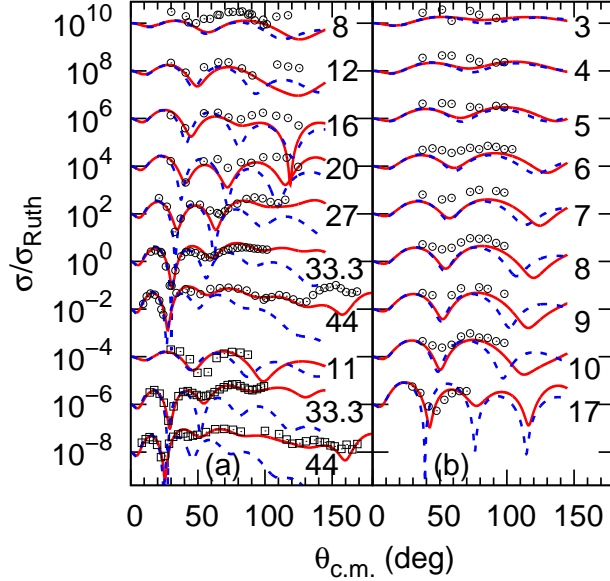


FIG. 4: (Color online) The same as in Fig. 2 but for ^3He elastic scattering from targets (a) ^6Li (circles) and ^7Li (squares), and (b) ^3H elastic scattering from ^6Li .

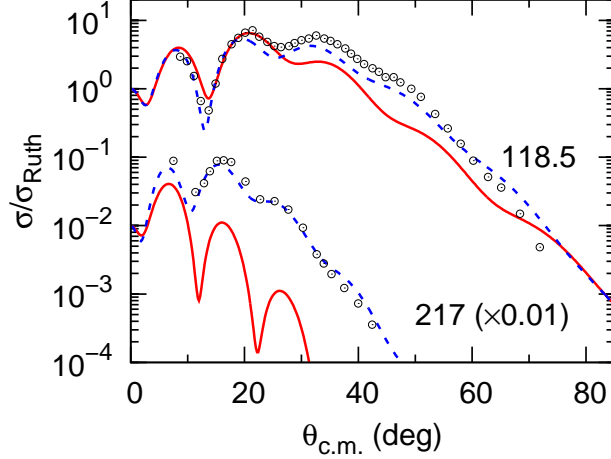


FIG. 5: (Color online) Comparison of the optical model calculations for ^3He elastic scattering from ^{12}C at 118.5 and 217 MeV with HT1p (solid curve) and GDP08 (dotted curve). The experimental data are from Refs. [33, 88].

understood from Trost et al. [26]. In Figs. 3 and 4 of Ref.[26], the authors show that the weak target-mass dependence assumed by GDP08 (only through the Coulomb corrections to the incident energies) is satisfied well at high energies. However, the target-mass dependence in the light-target region get stronger as incident energy decreases, what explains the failure of GDP08 at low energies.

B. Volume integrals of the OMPs

Volume integral per interacting nucleon pair of optical model potentials, denoted by J_v for the real part and J_w for the imaginary part, are important quantities to characterize different systematic potentials. These volume integrals are defined as:

$$\begin{aligned} J_v(E) &= \frac{1}{A_P A_T} \int V(E, r) d\vec{r}, \\ J_w(E) &= \frac{1}{A_P A_T} \int [W_v(E, r) + W_s(E, r)] d\vec{r}. \end{aligned} \quad (11)$$

J_v and J_w are supposed to be independent of the projectile and target masses, and are therefore useful to compare different systematic optical potentials. In Fig. 6 we compare the volume integrals of the potentials for ^3He impinging on ^{12}C from 1 to 220 MeV evaluated with HT1p and GDP08, respectively. As we discussed above, we estimate that HT1p is applicable for the $1p$ -shell nuclei below 100 MeV, while GDP08 is applicable at energies

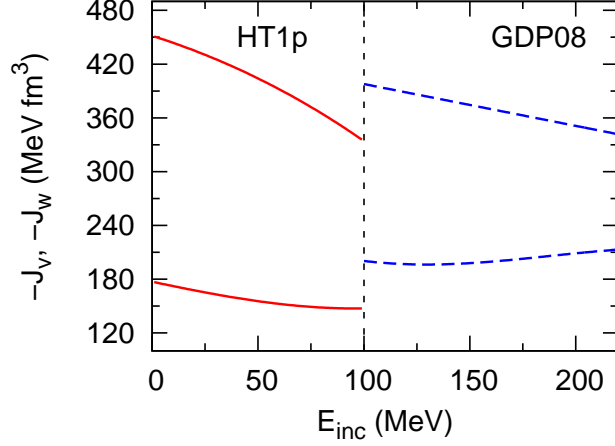


FIG. 6: (Color online) Volume integrals of the optical model potentials HT1p and GDP08 for ^3He elastic scattering from ^{12}C from 1 to 220 MeV. The vertical line divides the approximate energy regions in which HT1p and GDP08 are applicable for $1p$ -shell nuclei. The solid and dashed curves in the upper part of this figure represent the volume integrals of the real potentials of HT1p and GDP08, respectively. The curves in the lower part are for the corresponding imaginary potentials.

higher than this. Clearly, at energies around 100 MeV, there are abrupt differences in J_v and J_w between HT1p and GDP08. It indicates that new parameterization of the systematic potential should be made for the intermediate energy region to reconcile these two SOMPs, which are established individually in low- and high-energy regions. Experimental data of ^3He and ^3H elastic scattering from $1p$ -shell nuclei at ~ 100 MeV are therefore very much needed for such study.

IV. CONCLUSIONS

In conclusion, a set of global optical potential parameters for ^3He -nucleus elastic scattering, HT1p, is obtained by simultaneously fitting 118 sets of experimental data of ^3He and ^3H elastic scattering from $1p$ -shell nuclei from ^9Be to ^{18}O with incident energies from $4 \leq E \leq 118.5$ MeV and 24 sets of elastic scattering data with the ^6Li and ^7Li targets from $3 \leq E \leq 44$ MeV. This new systematic potential is found to be superior to GDP08, which is established for the heavy-target region, in reproduction of the angular distributions of the elastic scattering cross sections of ^3He and ^3H from $1p$ -shell nuclei at energies < 100 MeV. At energies above 100 MeV, GDP08 is found to be better than HT1p. Results of this paper can

pave the way to unify these two systematic potentials for a SOMP describing ^3He -nucleus elastic scattering in broad interval of energies.

Acknowledgements

DYP gratefully acknowledges the supports of the National Natural Science Foundation of China (Grant Nos. 11275018, 11035001, and U1432247) and the Chinese Scholarship Council (Grant No. 201303070253). W.D. acknowledges the support by the NSF under Grant No. PHY-1263281 (REU program). A. M. and DYP acknowledge that this material is based upon the work supported by the U.S. Department of Energy, Office of Science, Office of Nuclear Science, under Award Numbers DE-FG02-93ER40773 and DE-SC0004958. A.M. also acknowledges the support by the U.S. Department of Energy, National Nuclear Security Administration, under Award Number DE-FG52-09NA29467 and by the US National Science Foundation under Award PHY-1415656.

-
- [1] M.B. Tsang, Jenny Lee, and W.G. Lynch, Phys. Rev. Lett. 95, 222501 (2005).
 - [2] M.B.Tsang, J.Lee, S.C.Su, J.Y.Dai, M.Horoi, H.Liu, W.G.Lynch, and S.Warren, Phys. Rev. Lett. 102, 062501 (2009).
 - [3] Jenny Lee, Pang Dan-Yang, Han Yin-Lu, and M.B. Tsang, Chin. Phys. Lett. 31, 092103 (2014).
 - [4] J Dobaczewski, W Nazarewicz and P-G Reinhard, J. Phys. G: Nucl. Part. Phys. 41, 074001 (2014).
 - [5] X. D. Liu, M. A. Famiano, W. G. Lynch, M. B. Tsang, and J. A. Tostevin, Phys. Rev. C 69, 064313 (2004).
 - [6] F.D. Becchetti, Jr. and G.W. Greenless, Phys. Rev., **182**, 1209 (1969).
 - [7] R.L. Varner, W.J. Thompson, T.L. McAbee, E.J. Ludwig and T.B. Clegg, Physics. Reports. **201**, 57 (1991).
 - [8] A.J.Koning and J.P.Delaroche, Nucl. Phys. **A713**, 231 (2003).
 - [9] Ruirui Xu, Zhongyu Ma, E. N. E. van Dalen, and H. Müther, Phys. Rev. C 85, 034613 (2012).
 - [10] C.M. Perey and F.G. Perey, Phys. Rev. 132, 755 (1963).

- [11] J.M. Lohr and W. Haeberli, Nucl. Phys. A232, 381 (1984).
- [12] W.W. Daehnick, J.D. Childs, and Z. Vrcelj, Phys. Rev. **C21**, 2253 (1980).
- [13] Yinlu Han, Yuyang Shi, and Qingbiao Shen, Phys. Rev. C 74, 044615 (2006).
- [14] F. D. Becchetti, Jr., and G. W. Greenlees in *Polarization Phenomena in Nuclear Reactions* (H. H. Barschall and W. Haeberli, eds.) p. 682, The University of Wisconsin Press, Madison, Wis. (1971).
- [15] Hairui Guo, Yue Zhang, Yinlu Han, and Qingbiao Shen, Phys. Rev. C 79, 064601 (2009).
- [16] D.Y. Pang, P. Roussel-Chomaz, H. Savajols, R.L. Varner, and R. Wolski, Phys. Rev. **C79**, 024615 (2009).
- [17] Xiaohua Li, Chuntian Liang, Chonghai Cai, Nucl. Phys. **A789**, 103 (2007).
- [18] Chun-Tian Liang, Xiao-Hua Li and Chong-Hai Cai, J. Phys. G: Nucl. Part. Phys. 36, 085104 (2009).
- [19] T. Furumoto and Y. Sakuragi, Phys. Rev. C 74, 034606 (2006).
- [20] M. Avrigeanu, A. C. Obreja, F. L. Roman, V. Avrigeanu, and W. von Oertzen, At. Data Nucl. Data Tables 95, 501 (2009).
- [21] D.Y. Pang, Y.L. Ye and F.R. Xu, Phys. Rev. **C83**, 064619 (2011).
- [22] D.Y. Pang, Y.L. Ye, and F.R. Xu, J. Phys. G: Nucl. Part. Phys. **39**, 095101 (2012).
- [23] L. C. Chamon, B. V. Carlson, L. R. Gasques, et. al., Phys. Rev. C 66, 014610 (2002).
- [24] T. Furumoto, W. Horiuchi, M. Takashina, Y. Yamamoto, and Y. Sakuragi, Phys. Rev. C 85 044607 (2012).
- [25] Y. P. Xu and D. Y. Pang, Phys. Rev. C 87, 044605 (2013).
- [26] Hans-Jochen Trost, Peter Lezoch, and Udo Strohmusch, Nucl. Phys. A462, 333 (1987).
- [27] V. Lapoux, N. Alamanos, F. Auger et al., Phys. Lett. B517, 18 (2001).
- [28] D. Suzuki, H. Iwasaki, D. Beaumel, et al., Phys. Rev. Lett. 103 152503 (2009).
- [29] Fasial Jamil-Qureshi, Lou Jian-Ling, Ye Yan-Lin et al., Chin. Phys. Lett. 27, 092501 (2010)
- [30] B.A. Watson, P.P. Singh, and R.E. Segel, Phys. Rev. 182, 977 (1969).
- [31] L. Trache, A. Azhari, H.L. Clark, et al., Phys. Rev. C61, 024612 (2000).
- [32] P.P. Urone, L.W. Put, and B. W. Ridley, Nucl. Phys. A186, 344 (1972).
- [33] M. Hyakutake, I. Kumabe, M. Fukada, et al., Nucl. Phys. A333, 1 (1980).
- [34] B. Ja. Guzhovskij et al., Problemy Yadernoj Fiziki i Kosmicheskikh Luchej 7, 41 (1977). This data set is obtained from the EXFOR nuclear database sub-entry A0116001.

- [35] N.Otuka, E.Dupont, V.Semkova et. al., Nucl. Data Sheets 120, 272 (2014).
- [36] R.J. Eastgate, W.J. Thompson and R. A. Hardekopf, Comput. Phys. Commun., **5**, 69 (1973).
- [37] F. James and M. Roos, Comput. Phys. Commun. **10**, 343 (1975).
- [38] H. Lüdecke, Tan Wan-Tjin, H. Werner and J. Zimmerer, Nucl. Phys. A109, 676 (1968)
- [39] J.J. Schwartz, W.P. Alford, L.M. Blau and D. Cline, Nucl. Phys. 88, 539 (1966).
- [40] V. Burjan, J. Cejpek, J. Fojtu, et al., Phys. Rev. C 49, 977 (1994).
- [41] R.W. Givens, M.K. Brussel, and A.I. Yavin, Nucl. Phys. A187, 490 (1972)
- [42] W. Bohne, H. Homeyer, H. Lettau, et al., Nucl. Phys. A156, 93 (1970).
- [43] Gordon C. Ball and Joseph Cerny, Phys. Rev. 177, 1466 (1969).
- [44] A.K. Basak, O. Karban, S. Roman et al., Nucl. Phys. A368, 74 (1981)
- [45] G. Scheklinski, U. Strohmusch and B. Goel, Nucl. Phys. A153, 97 (1970).
- [46] A.S. Demijanov et al., Phys. Rev. C 38, 1975 (1988).
- [47] R. Görden, F. Hinterberger, R. Jahn, P. Von Rossen and B. Schüller, Nucl. Phys. A320, 296 (1979).
- [48] E.M. Kellogg, R.W. Zurmühle, Phys. Rev. 152, 890 (1966).
- [49] A.R. Kundson and F.C. Young, Nucl. Phys. A149, 323 (1970).
- [50] R.W. Zurmühle and C.M. Fou, Nucl. Phys. A129, 502 (1969).
- [51] H.M. Sen Gupta, J.R. Rotblat, E.A. King and J.B.A. England, Nucl. Phys. 50, 549 (1964).
- [52] W.S. McEver, T.B. Clegg, J.M. Joyce, E.J. Ludwig, and R.L. Walter, Nucl. Phys. A178, 529 (1972).
- [53] A.M. Mukhamedzhanov, et al., Phys. Rev. C 67, 065804 (2003).
- [54] J.Y. Park, J.L. Duggan, P.D. Miller et. al., Nucl. Phys. A134, 277 (1969).
- [55] S.I. Warshaw, A.J. Buffa, J.B. Barendt and M.K. Brussel, Nucl. Phys. A121, 350 (1968).
- [56] .G. Earwaker, Nucl. Phys. A90, 56 (1967).
- [57] A.J. Buffa, Jr. And M.K. Brussel, Nucl. Phys. A195, 545 (1972).
- [58] D.J. Baugh, G.J.B. Pyle, P.M. Rolph, and S.M. Scarrott, Nucl. Phys. A95, 115 (1967).
- [59] M.C. Lemaire, M.C. Mermaz, and Kamal K. Seth, Phys. Rev. C 5, 328 (1972).
- [60] W.E. Burcham, J.B.A England, R.G. Harris, O. Karban, and S. Roman, Nucl. Phys. A246, 269 (1975).
- [61] A. Garcia, J. Kirk, J.B.A. England, and P.E. Hodgson, Nucl. Phys. 38, 372 (1962).
- [62] P.V. Drumm, O. Karban, A.K. Basak, et al., Nucl. Phys. A448, 93 (1986).

- [63] J. Vernotte, G. Berrier-Ronsin, J. Kalifa, and R. Tamisier, Nucl. Phys. A390, 285 (1982).
- [64] J.L. Duggan, J.Y. Park, S.D. Danielopoulos, et al., Nucl. Phys. A151, 107 (1970).
- [65] R.L. Hutson, S. Hayakawa, M. Chabre et al., Phys. Lett. B27, 153 (1968).
- [66] .R. Patterson, J.M. Poate, B.A. Robson, and E.W. Titterton, Proc. Phys. Soc. 90, 577 (1967).
- [67] S.M. Barr and R.M. DelVecchio, Phys. Rev. C 15, 114 (1977).
- [68] L. Alvarez and G. Palla, J. Phys. G: Nucl. Phys. 8, 987 (1982).
- [69] J.H. Trost, A. Schwarz, U. Feindt, et al., Nucl. Phys. A337, 377 (1980).
- [70] G.T.A. Squier, E.A. McClatchie, A.R. Johnston, et al., Nucl. Phys. A119, 369 (1968).
- [71] Luisa F. Hansen, et al., Phys. Rev. 174, 1155 (1968).
- [72] A.S. Dem'yanova et al., Nucl. Phys. A542, 208 (1992).
- [73] P.M. Lewis, A.K. Basak, J.D. Brown, et al., Nucl. Phys. A395, 204 (1983).
- [74] H.R. Weller, N.R. Roberson, D.R. Tilley, Nucl. Phys. A122, 529 (1968).
- [75] P.D. Miller, J.L. Duggan, M.M. Duncan, et al., Nucl. Phys. A136, 229 (1969).
- [76] L.L. Green, C.O. Lennon and I.M. Naqib, Nucl. Phys. A142, 137 (1970).
- [77] M.A. M. Shahabuddin, C.J. Webb, V.R.W. Edwards, Nucl. Phys. A284, 83 (1977).
- [78] G.Thiamová, V. Burjan, J. Cejpek, V. Kroha, P. Navrátil, Nucl. Phys. A697, 25 (2002).
- [79] O. Aspelund, D. Ingham, A. Djalois, et al., Nucl. Phys. A231, 115 (1974).
- [80] L.A. Schaller, R.S. Thomason, N.R. Roberson, R.L. Walter, and R.M. Drisko, Phys. Rev. 163, 1034 (1967).
- [81] K.I. Pearce, N.M. Clarke, J.R. Griffiths, et al., J. Phys. G:Nucl. Phys. 12, 979 (1986).
- [82] J.B.A. England, L. Zybert, G.T.A. Squier et al., Nucl. Phys. A475, 422 (1987).
- [83] J.D. Sherman, E.R. Flynn, Nelson Stein, J.W. Sunier and D.G. Burke, Phys. Rev. C 13, 2122 (1976)
- [84] P.J. Simmonds, K.I. Pearce, P.R. Hayes, et al., Nucl. Phys. A482, 653 (1988).
- [85] P.W. Keaton Jr., D.D. Armstrong, L.R. Veaser, et al., Nucl. Phys. A179, 561 (1972).
- [86] A.S. Demiyanova H. G. Bohlen, B. Gebauer et al., Nucl. Phys. A553, 727c (1993).
- [87] B. Efron, Biometrika 68 (1981) 589; *ibid.*, SIAM Rev. 21(1979) 460, and P. Diaconis and B. Efron, Sci. Am. 248, 116 (1983).
- [88] N. Willis, I. Brissaud, Y. Le Bornec, B. Tatischeff, and G. Duhamel, Nucl. Phys. **A204**, 454 (1973).